Cell-Based Region Competition for Ultrasound Image Segmentation

Chung-Ming Chen* Henry Horng-Shing Lu[1] Bin-Shin Su[1]

Institute of Biomedical Engineering, National Taiwan University, Taipei, Taiwan, 100, ROC
[1]Institute of Statistics, National Chiao-Tung University, Hsinchu, Taiwan,300, ROC

Received 20 May 2002; Accepted 7 June 2002

Abstract

A new approach, cell-based region competition, based on watershed transform and region competition is proposed to detect the multiple objects of interest with highly winding contours in the ultrasound images. Multi-scale Gaussian filters are used to remove the speckle in the ultrasound image and preserve the edge information. Sobel filter are then applied to generate a gradient map. Immersion simulation of watershed transform is used to generate initial cells on the gradient map. Cell-based region merging and splitting are performed on the original ultrasound images based on the likelihood ratio tests of speckle noises. Two types of images have been used to evaluate the performance of the proposed cell-based region competition scheme, namely, the simulated phantom images with the speckle and the clinical ultrasound images. The experimental results on both types of images demonstrate the practical feasibility of the proposed cell-based region competition scheme for ultrasound image segmentation.

***Keywords*:** Ultrasound Image Segmentation, Region Competition, Watershed Transform, Multi-scale Gaussian filtering, Winding Contour

Introduction

Ultrasonic imaging is a prevailing imaging modality nowadays due to its properties of non-invasion, real-time, convenience, and economy. While quantitative ultrasound image analysis highly relies on the extraction of the objects of interest from the images, segmenting the objects of interest in an ultrasound image is very difficult because of the speckle, the tissue related textures and artifacts. Some typical segmentation tasks are 3D reconstruction, tumor volume estimation, ovarian follicle size measurement, and so on. To overcome the complex nature of the ultrasound images, varieties of segmentation techniques have been proposed previously for specific applications. As an example, Krivanek et al. [1] employed watershed segmentation and a knowledge-based graph search algorithm to measure the size and the shape of ovarian follicles. For accurate detection of the lumen-intima and media-adventitia boundaries, Fan [2] applied a nonlinear wavelet soft thresholding algorithm to intracoronary ultrasound images.

At least three classes of approaches have been suggested for segmentation of general ultrasound images. One is trying to eliminate the speckle first, followed by classic segmentation schemes [3]. Another is to employ the texture image segmentation techniques by considering ultrasound images as texture images [4]. The other is to adopt the deformable model, e.g., the snake model, to find out the boundary of the object of interest [5-6]. Most of these approaches have been designed to segment one object of interest at a time. Effective as they are, they might not be applicable to two types of analysis problems. One is to find the boundary of the object of interest without the prior knowledge of the object position. The other is to extract multiple objects of interest in an image simultaneously, especially, when the boundary is highly winding.

These two problems may be resolved by using such region-based approaches as split-and-merge, region competition, and so on. However, the conventional split-and-merge type approaches share the common deficiency that once one block of subimage is merged into some segment, it cannot be reassigned to some other segment. Although this deficiency may be remedied by the region competition technique, the pixel-based or small-region based competition involved in the conventional regional competition algorithms [7-8] tend to be statistically unreliable because of the low signal-to-noise ratio inherently in an ultrasound image. Alternatively, in this paper, we present a new approach, called cell-based region competition, for ultrasound image segmentation. The basic idea of the proposed approach is to decompose the underlying image into cells with similar image property and combine the cells into regions, each of which may comprise more than one cell. Algorithmically, the first step is to apply multi-scale Gaussian filters to remove the

* Corresponding author: Chung-Ming Chen
Tel: +886-2-23630231 ext. 3953; Fax: +886-2-23940049
E-mail: ming@lotus.mc.ntu.edu.tw

speckle noises and preserve edge information. Then, filters, like the Sobel filter, are used to estimate the gradient vectors. With the gradient vectors, an initial segmentation is generated by the watershed transform [9-11]. These initial regions are further combined by the technique of region competition [7-8] based on likelihood ratio tests among cells.

This paper is organized as follows. Section 2 describes the basic techniques employed in this study, including the watershed transform and the region competition. Section 3 presents the proposed cell-based region competition. The experimental results and discussions using the simulated and the clinical ultrasound images are provided in Section 4. The conclusions are given in Section 5.

Watershed Transform and Region Competition

The watershed transform is employed to identify the edges defined by the local maxima in the gradient map of the ultrasound image, which may be generated by using any gradient-type filter, e.g., the Sobel operator. The watershed transform may be realized by two different approaches, namely, the rainfall [11] and the immersion [9] simulation. The idea of the rainfall method is to simulate the way that rains flow into the dales along the directions of the gradient vectors. The boundaries of different flowing directions of rainfalls define the watersheds. On the other hand, in the immersion method, the gradient map is viewed as a landscape made up of catchment basins of various sizes and shapes. Each catchment basin has a hole at the bottom, which is defined by the minimum gradient value within the catchment basin. One may imagine when the gradient map is immersed into water, the water will start to permeate into the catchment basins from the one with the lowest bottom. As the water levels increases, the watersheds are defined where the water in the adjacent catchment basins merges. Fig. 1 illustrates two catchment basins with water of the same level. The peak between two catchment basins will be where the water will meet when the water level goes high enough, which defines the watershed.

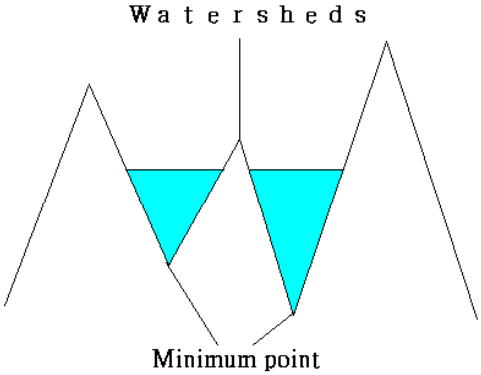

Figure 1. An illustration of building a watershed where the water between two catchment basins meets.

The technique of region competition was proposed by Zhu and Yullie [7], which was based on a global energy that consists of a log-likelihood and an arc-length terms. Suppose the original ultrasound image R, not the smoothed image, is decomposed into M distinct regions $R_i, i = 1,2,...,M$. The energy function is

$$E(\Gamma, \{\sigma_i\}) = \sum_{i=1}^{M} \{\frac{u}{2} \oint_{\partial R_i} ds - \log P(R_i \mid \sigma_i)\} \quad (1)$$

where $\Gamma_i = \partial R_i$ is the boundary of R_i, $\Gamma = \cup \Gamma_i$ is the total boundaries, σ_i is the model parameter set, $\log P(R_i \mid \sigma_i)$ is the log-likelihood of the pixels in region R_i and $u > 0$ is a weighting factor, which is determined empirically. Let n_i be the number of pixels in region i and the intensity for each pixel j in region i be I_j. Suppose the intensities are independently and identically distributed as a Rayleigh distribution [12-13] with a parameter $\sigma_i > 0$, the probability density function for I_j is

$$P(I_j \mid \sigma_i) = \frac{I_j}{\sigma_i^2} e^{\frac{-I_j^2}{2\sigma_i^2}}. \quad (2)$$

Thus, the likelihood of region i is

$$P(R_i \mid \sigma_i) = \prod_{j=1}^{n_i} P(I_j \mid \sigma_i) = \prod_{j=1}^{n_i} \frac{I_j}{\sigma_i^2} e^{\frac{-I_j^2}{2\sigma_i^2}}. \quad (3)$$

The maximum likelihood estimate (MLE) of σ_i of region i turns out to be

$$\hat{\sigma}_i = \sqrt{\frac{\sum_{j=1}^{n_i} I_j^2}{2n_i}}. \quad (4)$$

The basic idea of region competition is to perform the likelihood ratio tests between neighboring regions. When the pixel $\vec{v} = (x, y)$ locates at the common boundary of region i and region j, the steepest descent direction of the energy function by variational techniques is

$$\frac{d\vec{v}}{dt} = -uk_i(\vec{v})\vec{n}_i(\vec{v}) + [2\log(\frac{\hat{\sigma}_j}{\hat{\sigma}_i}) - I(\vec{v})(\frac{1}{2\hat{\sigma}_i^{\,2}} - \frac{1}{2\hat{\sigma}_j^{\,2}})]\vec{n}_i(\vec{v}) \quad (5)$$

where $k_i(\vec{v})$ is the curvature of Γ_i at $\vec{v}$, $\vec{n}_i(\vec{v})$ is the unit normal vector that points outward region i at $\vec{v}$, $\hat{\sigma}_i$ is the MLE of region i, and $\hat{\sigma}_j$ is the MLE of region j. The second term in Eq. (5) is a likelihood ratio test. If the pixel $I(\vec{v})$ has higher likelihood in region i, then $\vec{v}$ moves along $\vec{n}_i$ and the pixel is included in region i. The first term is a regularization term against the large value of curvature.

The Cell-based Region Competition

The proposed cell-based region competition approach is depicted in Fig. 2. Multi-scale Guassian filters are first used to smooth the initial image and preserve the edge information.

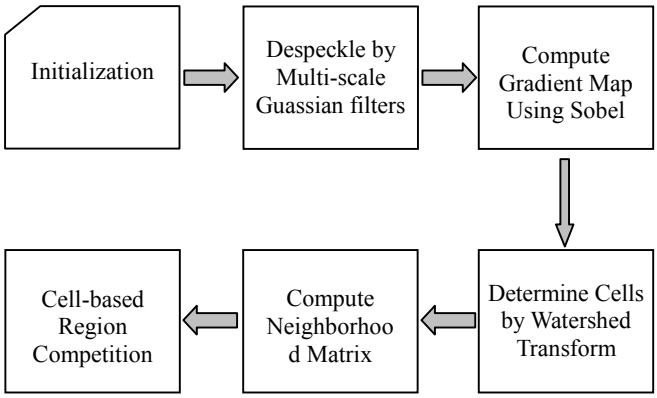

Figure 2. The block diagram of the proposed cell-based region competition approach.

Sobel filters are then used to generate the gradient map that consists of the absolute values of gradient vectors. Immersion simulation is used to produce the watershed transform that generates initial cells. Neighboring relationships of initial cells are stored in a neighborhood matrix. Cells are combined into regions and regions may be further split. The merging and splitting are based on the likelihood ratio tests of the original ultrasound images. The neighborhood matrix is updated and merging/splitting iterates until stopping criteria are met.

3.1. Neighborhood Matrix

The initial cells are generated after the watershed transform. When two or more cells are merged, it is called a region. If a region consisting of two cells is split, this region dismissed. To keep tracking the neighboring relationship of these cells and regions as the cell-based split and merge proceeds, a neighborhood matrix is constructed to record the relations among adjacent cells and regions. Let A denote the neighborhood matrix. If cells (or regions) *i* and *j* are next to each other, $a_{ij} = a_{ji} = 1$. Otherwise, $a_{ij} = a_{ji} = 0$. The diagonal entries are set to be zeros, i.e., $a_{ii} = 0$. Thus, the neighborhood matrix is a symmetric matrix with entries of 0 or 1. For instance, Fig. 3(a) illustrates an image with 6 cells and Fig. 3(b) the associated neighborhood matrix. If cell 2 is merged with cell 3, the new neighborhood matrix is displayed in Fig. 4. The new region consists of cells 2 and 3 are labeled as region 2 as shown in Fig. 4(a). Therefore, there will be one region and four cells left in this case. A new 5 by 5 neighborhood matrix is generated for the remaining one region and four cells.

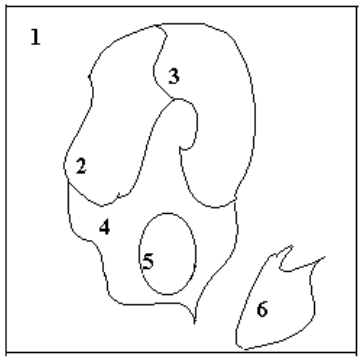

(a)

	1	2	3	4	5	6
1	0	1	1	1	0	1
2	1	0	1	1	0	0
3	1	1	0	1	0	0
4	1	1	1	0	1	0
5	0	0	0	1	0	0
6	1	0	0	0	0	0

(b)

Figure 3. (a) An example of an image with 6 cells, and (b) the associated neighborhood matrix.

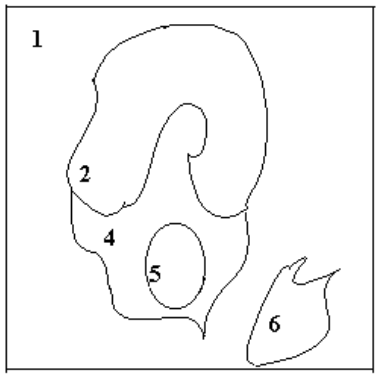

(a)

	1	2	4	5	6
1	0	1	1	0	1
2	1	0	1	0	0
4	1	1	0	1	0
5	0	0	1	0	0
6	1	0	0	0	0

(b)

Figure 4. (a) An illustration of merging cells 2 and 3, resulting region 2, and (b) the associated neighborhood matrix

3.2. Cell-based Split-and-Merge

Three types of splitting and merging have been considered in this studied. These three types are Types Ⅰ, Ⅱ, and Ⅲ, which represent competition between two cells, one cell and one region, as well as one region and one cell in another region, respectively.

3.2.1. Type Ⅰ

For instance, cells 2 and 3 in Fig. 3 may be merged into a new region. Suppose that cells 2 and 3 may be haracterized by the probability distributions, e.g., the Rayleigh

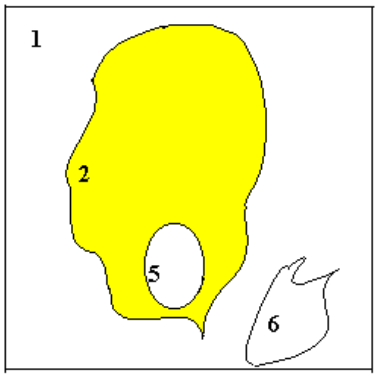

Figure 5. An illustration for merging cell 4 into region 2.

distributions, with parameters σ_2 and σ_3. Then the null and alternative hypotheses are

$$H_0 : \sigma_2 = \sigma_3 \quad vs. \quad H_1 : \sigma_2 \neq \sigma_3$$

If the null hypothesis is not rejected, cells 2 and 3 are merged into a new region, which is labeled as region 2, as shown in Fig. 4.

3.2.2. Type Ⅱ

For example, region 2 and cell 4 in Fig. 4 may be merged to form a bigger region 2, which is shown as a dark region in Fig. 5. Suppose that region 2 and cell 4 have probability distributions with parameters σ_2 and σ_4.

$$H_0 : \sigma_2 = \sigma_4 \; vs. \; H_1 : \sigma_2 \neq \sigma_4$$

The hypothesis testings for two cells and one cell and one region are similar. However, there is no new region generated for one cell and one region.

3.2.3. Type Ⅲ

Suppose that cells 1 and 6 in Fig. 5 are merged to form a new region, named as region 1. Then, cell 4 may be split from region 2 and merged into region 1. This is necessary because this new merging and splitting may provide better segmentation results. If cell 4 is split from region 2, the new region 2 only consists of cells 2 and 3. The parameters of probability distributions in cell 4, new region 2 (of cell 2 and 3), and region 1 (of cell 1 and 6) are estimated and denoted as σ_4, σ_2 and σ_1 respectively. The following two hypotheses are considered. The first one considers merging cell 4 to region 1 as follows:

$$H_0 : \sigma_4 = \sigma_1 \; vs. \; H_1 : \sigma_4 \neq \sigma_1.$$

The other hypothesis considers the merging of cell 4 to the new region 2, i.e., keeping cell 4 in the region consisting of cells 2 and 3:

$$H_0 : \sigma_4 = \sigma_2 \; vs. \; H_1 : \sigma_4 \neq \sigma_2.$$

If the first one has the higher likelihood ratio test statistics, cell 4 is split from region 2 and merged into region 1. Otherwise, cell 4 remains in region 2. The cycling phenomena may occur. For example, cell 4 may be split from region 2 in one time and merged back into region 2 in another time. We will record the number of times that cell 4 is merged into region 2. If cell 4 is merged into region 2 for the second time, then cell 4 will be

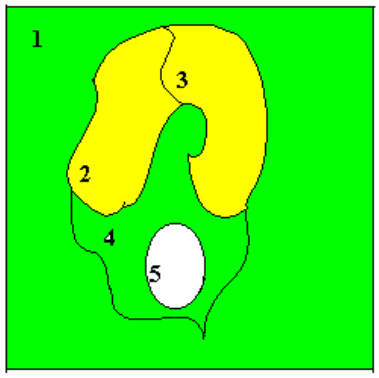

Figure 6. Cell 4 is split from region 2 (the light gray area) and merged into region 1 (the dark gray area).

kept at region 2 thereafter in our current approach. Figure 6 shows the case that cell 4 is split from region 2 (defined as the light gray area) and merged into region 1 (defined as the dark gray area). Note that cell 6, which is not shown in Fig. 6, has been combined with cell 1, resulting region 1.

3.3. Stepwise Merging/Splitting

There are a variety of possible merging and splitting for all the initial cells generated by the watershed transform. In order to decide which merging and splitting shall be preformed first, we use stepwise merging/splitting. That is, at each time, we only choose one merging/splitting among all possible cases belonging to Types Ⅰ, Ⅱ, and Ⅲ. This is selected by the maximum value of the likelihood ratio test statistics by exhaustive search among all possible merging/splitting of one cell.

For instance, we can use the Rayleigh distribution for modeling of speckle noises in ultrasound images. The probability distribution is given in Eq. (2) and the maximum likelihood estimate (MLE) is shown in Eq. (4). For the hypothesis testing of one cell, R_i, to the other cell (or region), R_j, the following likelihood ratio test is used. The number of pixels in R_i and R_j are denoted as n_i and n_j. The estimated parameters are assumed to be σ_i and σ_j. The null and alternative hypotheses are $H_0 : \sigma_i = \sigma_j = \sigma$ *vs.* $H_1 : \sigma_i \neq \sigma_j$. Under H_0, the likelihood becomes

$$\begin{aligned} L(\sigma \mid R_i, R_j) &= P(R_i \mid \sigma) P(R_j \mid \sigma)) \\ &= \prod_{k=1}^{n_i} P(I_k \mid \sigma) \prod_{l=1}^{n_j} P(I_l \mid \sigma) \\ &= \sigma^{-2(n_i+n_j)} \exp\{-\frac{\sum_{k=1}^{n_i} I_k^2 + \sum_{l=1}^{n_j} I_l^2}{2\sigma^2}\} \prod_{k=1}^{n_i} I_k \prod_{l=1}^{n_j} I_l. \end{aligned} \tag{6}$$

The MLE of σ under H_0 turns out to be

$$\hat{\sigma} = \sqrt{\frac{\sum_{k=1}^{n_i} I_k^2 + \sum_{l=1}^{n_j} I_l^2}{2(n_i + n_j)}}. \tag{7}$$

Under H_1, the likelihood is

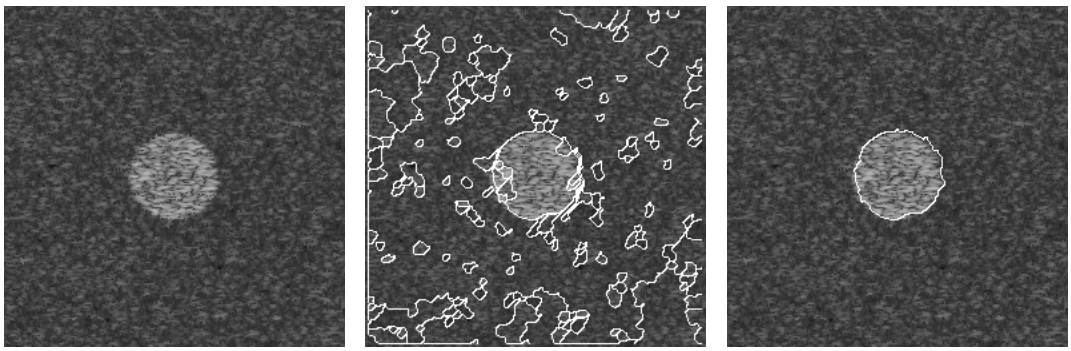

Figure 7. Performance demonstration for the simulated phantom image with SNR=2, in which the left image is the test image and the central disc is the object of interest, the middle image shows the initial cells by watershed transform, and the right image is the segmentation result by the proposed cell-based region competition.

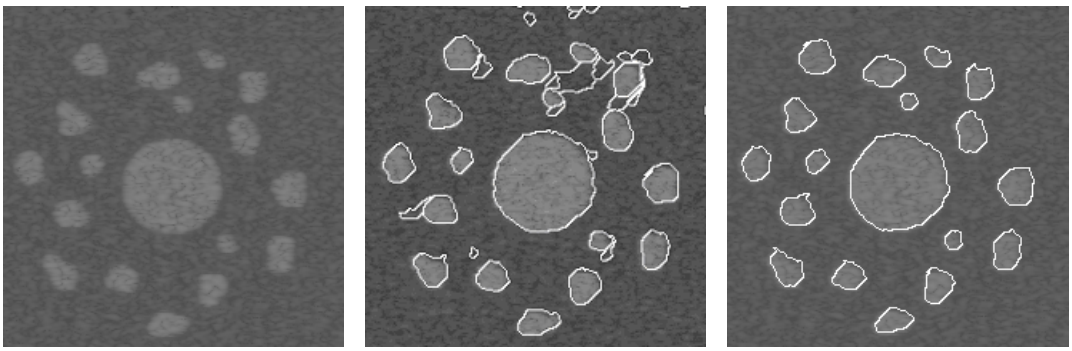

Figure 8. Performance demonstration for the simulated phantom image with SNR=6, in which the left image is the test image and the central disc is the object of interest, the middle image shows the initial cells by watershed transform, and the right image is the segmentation result by the proposed cell-based region competition.

$$
\begin{aligned}
L(\sigma_i,\sigma_j \mid R_i,R_j) &= P(R_i \mid \sigma_i)P(R_j \mid \sigma_j) \\
&= \prod_{k=1}^{n_i} P(I_k \mid \sigma_i)\prod_{l=1}^{n_j} P(I_l \mid \sigma_j) \\
&= \sigma_i^{-2n_i}\sigma_j^{-2n_j}\exp\{-(\frac{\sum_{k=1}^{n_i} I_k^2}{2\sigma_i^2}+\frac{\sum_{l=1}^{n_j} I_l^2}{2\sigma_j^2})\}\prod_{k=1}^{n_i} I_k \prod_{l=1}^{n_j} I_l
\end{aligned}
\tag{8}
$$

The MLE of σ_i becomes

$$
\hat{\sigma}_i = \sqrt{\frac{\sum_{k=1}^{n_i} I_k^2}{2n_i}}, \tag{9}
$$

and the MLE of σ_j turns out to be

$$
\hat{\sigma}_j = \sqrt{\frac{\sum_{l=1}^{n_j} I_l^2}{2n_j}}. \tag{10}
$$

Therefore, the likelihood ratio test statistic is

$$
\begin{aligned}
\lambda(R_i,R_j) &= \frac{L(\hat{\sigma} \mid R_i,R_j)}{L(\hat{\sigma}_i,\hat{\sigma}_j \mid R_i,R_j)} \\
&= (\frac{\hat{\sigma}_i}{\hat{\sigma}})^{2n_i}(\frac{\hat{\sigma}_j}{\hat{\sigma}})^{2nj}\exp\{\frac{(\hat{\sigma}^2-\hat{\sigma}_i^2)\sum_{k=1}^{n_i} I_k^2}{2\hat{\sigma}^2\hat{\sigma}_i^2}+\frac{(\hat{\sigma}^2-\hat{\sigma}_j^2)\sum_{l=1}^{n_j} I_l^2}{2\hat{\sigma}^2\hat{\sigma}_j^2}\}.
\end{aligned}
\tag{11}
$$

The larger the ratio is, the more likely these two cells (or regions) shall be merged. Therefore, we will compute the likelihood ratio test statistics for all possible cases and select that one has the largest value to merge and split.

After this iterative procedure completes, all cells will be merged into different regions. Then, these regions will be regarded as new cells and further merging/splitting process can repeat. This kind of repetition will stop when the largest value of likelihood ratio test statistics is smaller than a predefined threshold.

Experimental Results and Discussions

The simulation studies will investigate the performance of the proposed cell-based region competition on the simple phantoms with the speckle of Rayleigh distributed. The signal-to-noise ratio (SNR) is defined to be the ratio of the signal and the noise levels. The signal level is defined to be the difference between the mean intensities of the object and the background. The noise level is set to be the standard deviation of the speckle. The clinical studies will explore the performance of the proposed cell-based region competition on clinical ultrasound images collected at National Taiwan University Hospital (NTUH).

4.1 Studies on the Simulated Phantom Images

Two simulation studies are displayed in Figs. 7 and 8. The first phantom shown in Fig. 7 is only a circle in the region of interest (ROI) and the SNR is 2. The second phantom in Fig. 8 comprises a circle as the ROI and other small objects in

the background with the SNR equal to 6. The initial cells generated by the watershed transform are displayed in the middle in both figures. These over-segmented initial cells can be merged and split by the proposed cell-based region competition to reach the final segmentation in the right figures. Not only the ROI but also the other small objects are successfully segmented by this new approach. In addition, the final segmentation results are quite close to the target boundaries. These establish the foundation for further applications in clinical ultrasound images.

4.2 Studies on the Clinical Images

For the succinctness of presentation, the segmentation results for four clinical ultrasound images are provided in Figs. 9-12. Figs. 9 and 10 are liver ultrasound images and Figs. 11 and 12 are breast ultrasound images. For all these four images, the test images are in the left, the initial cells derived by the watershed transform are shown in the middle and the segmentation results by the proposed cell-based region competition are demonstrated in the right. The over-segmentation results by the watershed transform in the middle are reduced by the proposed cell-based region competition in the right. This new method locates not only the concave boundaries of ROI but also other concave boundaries in the background. For example, the proposed approach has successfully identified the winding contour of the lower-right portion of the breast lesion in Fig. 11, which is not easily captured by the conventional schemes, e.g., the deformable models. The final segmentation boundaries of ROI are quite close to the target ones. These demonstrate the feasibility of this new approach for clinical ultrasound images.

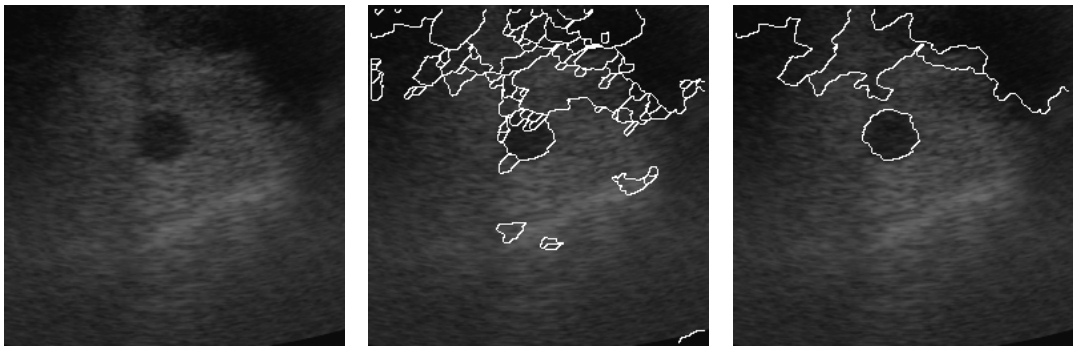

Figure 9. Performance demonstration for the first liver ultrasound image, in which the left image is the test image, the middle image shows the initial cells by watershed transform, and the right image is the segmentation result by the proposed cell-based region competition.

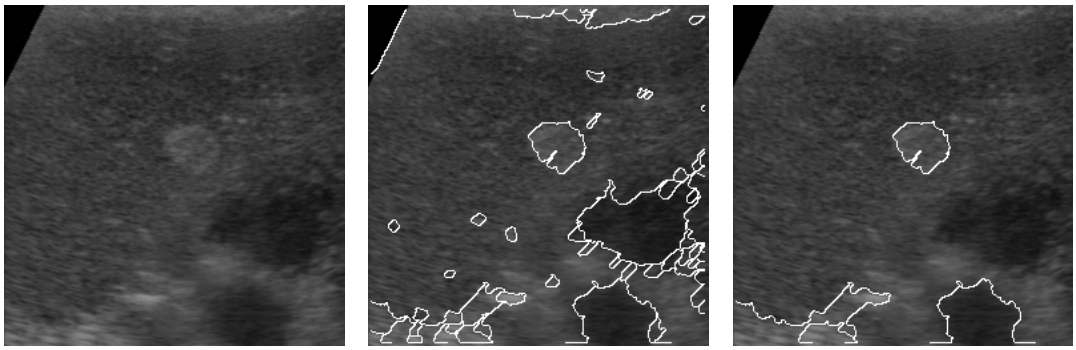

Figure 10. Performance demonstration for the second liver ultrasound image, in which the left image is the test image, the middle image shows the initial cells by watershed transform, and the right image is the segmentation result by the proposed cell-based region competition.

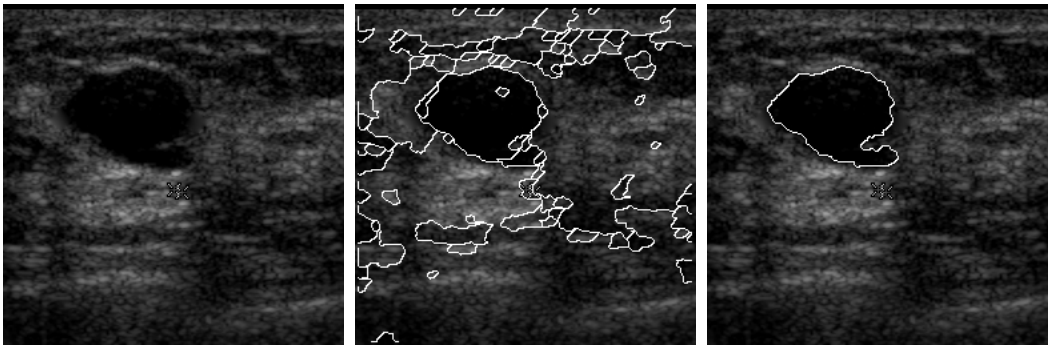

Figure 11. Performance demonstration for the first breast ultrasound image, in which the left image is the test image, the middle image shows the initial cells by watershed transform, and the right image is the segmentation result by the proposed cell-based region competition.

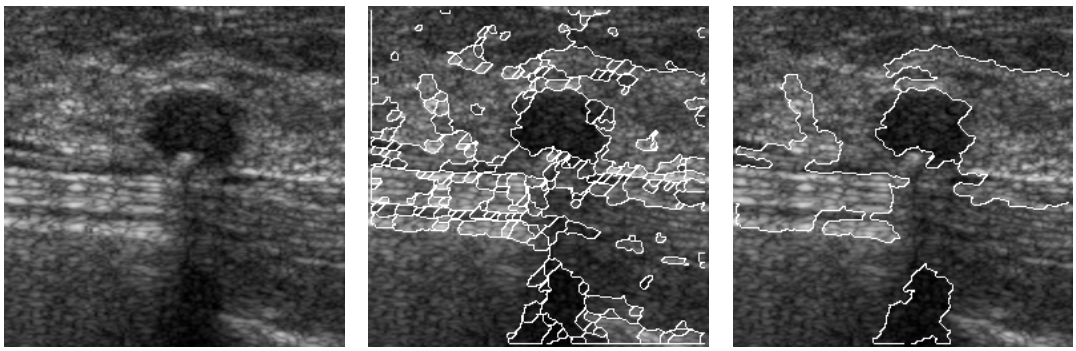

Figure 12. Performance demonstration for the second breast ultrasound image, in which the left image is the test image, the middle image shows the initial cells by watershed transform, and the right image is the segmentation result by the proposed cell-based region competition.

Conclusions

To identify the multiple objects of interest with highly winding contours, in this paper, a new approach, namely, cell-based region competition, has been proposed for ultrasound image segmentation. The basic idea of the proposed scheme is to decompose the image into cells of homogeneous area and use cell-based split-and-merge approach to combine the cells. The cells are generated by the watershed transform using the immersion simulation method. By incorporating regional information in cells of the original ultrasound images, this cell-based approach can detect multiple concave boundaries effectively as demonstrated in the experimental studies using the simulated phantom images and the clinical ultrasound images. Promising as it is, this scheme should be further verified by the quantitative analysis, e.g., evaluating the performances in terms of the distances between the desired and the derived boundaries, in more thorough experimental studies. More sophisticated methods to handle or remove cycling phenomena inherent in the cell-based region competition are useful to improve the performance. Stopping criterion for the iterative process of merging/splitting is another crucial factor for the practicability of the proposed algorithm.

Reference

[1] A. Krivanek, W. Liang, G. E. Satry, R. A. Pierson and M. Sonka, "Automated follicle analysis in ovarian ultrasound", *Proc. SPIE Int. Symp. Medical Imaging*, 1998, vol.3338, 588-596.

[2] L. Fan, G. A. Braden and D. M. Herrington, "Nonlinear wavelet filter for intracononary ultrasound images", *Proc. of the 23rd Annual Meeting on Comp. in Cardiology*, 1996, 41-44.

[3] C. Kotropoulos, "Nonlinear ultrasonic image processing based on signal-adaptive filters and self-organizing neural networks", *IEEE Trans. Image Processing*, 3: 65-77, 1994.

[4] R. Muzzolini, Y. H. Yang and R. Pierson "Texture characterization using robust statistics", *Pattern Recognition*, 27: 119-134, 1994.

[5] V. Chalana, D. T. Linker, D. R. Haynor and Y. Kim, "A multiple active contour model for cardiac boundary detection on echocardiographic sequences", *IEEE Trans. Med. Imaging*, 15: 290-298, 1996.

[6] C.M. Chen, H. H.-S. Lu, and A.T. Hsiao, "A Dual Snake Model of High Penetrability for Ultrasound Image Boundary Extraction", *Ultrasound in Medicine and Biology*, 27: 1651-1665, 2001.

[7] S. C. Zhu and A. Yuille, "Region competition: unifying snakes, region growing, and Bayes/MDL for multiband image segmentation", *IEEE Trans. PAMI*, 18: 884-900, 1996.

[8] C. M. Chen, H. H-S. Lu, and Y.-L. Chen, "A discrete region competition approach incorporating weak edge enhancement for ultrasound image segmentation", *Pattern Recognition Letters*, in press, 2001.

[9] L. Vincent and P. Soille. "Watersheds in digital spaces: an efficient algorithm based on immersion simulation", *IEEE Trans. PAMI*, 13:583-597, 1991.

[10] K. Haris, S. N. Efstratiadis, N. Maglaveras, A. K. Katsaggelos, "Hybrid image segmentation using watersheds and fast region merging", *IEEE Trans. Image Processing*, 7: 1684-1699, 1998.

[11] J. M. Gauch, "Image segmentation and analysis via multiscale gradient watershed hierarchies", *IEEE Trans. Image Processing*, 8: 69-79, 1999.

[12] C. B. Burckhardt, "Speckle in ultrasound B-mode scans", *IEEE Trans. Ultrasonics*, 25: 1-6, 1978.

[13] Goodman, J. W., 1985. Statistical Optics. Wiley, New York.